nature communications

Article

https://doi.org/10.1038/s41467-025-60972-2

Coral growth records 20th Century sea-level acceleration and climatic variability in the Indian Ocean

Received: 2 November 2024

Accepted: 10 June 2025

Published online: 01 July 2025

Check for updates

Paul S. Kench[1] ✉, Kyle M. Morgan[2,3], Susan D. Owen[1], Ke Lin[2], Xianfeng Wang[2,3] & Riovie D. Ramos[2]

Empirical observations of the rate of sea-level rise (SLR) and the timing of its recent acceleration are critical for validating ensemble methods used to determine global mean sea level trends. Such records are critically important at far-field locations where instrumental datasets are scarce. Here we construct a continuous 90-year sea level record (1930–2019) from the central tropical Indian Ocean derived from the incremental growth of a coral microatoll, which is demonstrated to reflect changes in sea level at annual timescales. Our record, which overlaps with tide gauge observations, extends the instrumental record by six decades and reveals climatic variability and marked changes in sea level behaviour across the twentieth century characterised by: (1) an increase in sea level of 0.30 m between 1930 and 2019; (2) low rates of SLR in the early twentieth century (1.42 ± 0.42 mm.yr^{-1}); (3) a marked acceleration in SLR to ~3.44 ± 0.68 mm.y^{-1} in the late 1950's; and (4) a further increase to 4.39 ± 0.48 mm.y^{-1} over the past three decades. Our results provide empirical evidence for a mid-century SLR acceleration in the central Indian Ocean, which is earlier than instrumental records indicate for coastal sites at the continental margins.

Observational records of 20thcentury global mean sea level (GMSL) change are essential to improve our understanding of climate change and natural climatic variability[1]. Historical records allow for assessment of the current state of the climate system and changes over time, improving knowledge of regional and global sea level variability. In addition, they enable the evaluation of climate and earth systems models[2,3] and play a crucial role in quantifying the socio-economic impacts of sea-level change on vulnerable coastal communities and ecosystems worldwide[4].

Observational sea level records have been successfully used to validate synthesised sea level records at both global and regional scales[2,3]. These studies show good agreement in the period since satellite altimetry data of ocean water level has been available, and confirm that the pace of sea level change has accelerated since 1993[5,6]. However, there are greater disparities between models and tide gauge observations in the twentieth century prior to the availability of satellite data[3]. Indeed, it has been shown that the recent increase in rate of sea-level rise was not a recent phenomenon that was coincident with satellite altimetry data, but had been underway for several decades[4]. Furthermore, regional sea level reconstructions based on tide gauge records show sea-level change has substantial regional departures from the GMSL at decadal to multidecadal timescales[3]. Comparison of ocean reanalysis products that reconstruct patterns and trends in sea surface height over the past 60 years also shows significant disagreement between models prior to the satellite altimeter record[7].

Several factors account for such disparities in the pattern of estimated past sea level change. First, there are very few instrumental sea-level records of sufficient length (>70 years) to detect long-term trends[8,9]. Second, the spatial distribution of these records is mostly

[1]Department of Geography, National University of Singapore, Singapore, Singapore. [2]Earth Observatory of Singapore, Nanyang Technological University, Singapore, Singapore. [3]Asian School of the Environment, Nanyang Technological University, Singapore, Singapore. ✉e-mail: pkench@nus.edu.sg

concentrated at coastal sites in the northern hemisphere, while large tracts of major ocean basins within far-field locations have few, if any, instrumental observations to resolve long-term sea-level behaviour. This lack of observational data is particularly acute in the Southern Ocean and mid-ocean basins[7]. Third, coastal records are beset with numerous confounding factors associated with the dynamical response of the ocean to atmospheric forcing, their interaction with shallow coastal shelves, terrestrial runoff and water storage, and vertical land motion[3]. While advances have been made to resolve a number of the above issues in closure of the 20th century sea level budget[10–12], significant gaps in observational data remain.

The Indian Ocean has only two long sea-level records that span the twentieth century, located on the northwestern coastline of India (Mumbai, PMSL Station ID 43, 142 years) and the southwestern coast of Australia (Fremantle, PMSL Station ID 111, 124 years), which are 7300 km apart. In contrast, instrumental observations at central tropical locations in the Indian Ocean are only 3-4 decades in length (Supplementary Table 1 and Supplementary Fig. 1). These short records indicate rates of sea-level rise between 3.37 ± 0.05 and 7.06 ± 0.76 mm.yr^{-1} over the past three decades, though are not able to shed light on the timing of the acceleration in sea level change, or variations in the pattern of sea level change in the tropical Indian Ocean across the twentieth century. Tide gauge reconstruction and ocean assimilation analysis have also shown equivocal and contrasting results for the central Indian Ocean since 1960[7] and significant spatial variation[13]. The lack of observational data within the Indian Ocean inhibits the ability to verify sea-level reconstructions based on statistical and reanalysis techniques. Consequently, the current absence of extended historical records represents a significant gap in the improved understanding of sea-level behaviour, including recent accelerations and rates of rise, in the central Indian Ocean[14]. Such data is critical in the region given the abundance of low-lying coastal areas, and islands, and heightened vulnerability of coastal communities and coastal ecosystems in the Indian Ocean[15–17].

In the absence of long-term instrumental records, reconstructions of relative sea-level (RSL) can be derived using sea-level proxies. Such proxies include sedimentary deposits, geomorphic features, fixed biological indicators, corals, and salt marsh systems[18]. Each proxy has a systematic and quantifiable relationship to sea-level, and they have been adopted to resolve sea-level behaviour over a range of geological timescales spanning the mid-Pliocene warm period, last interglacial, and across the recent Holocene postglacial sea-level transgression[18]. The utility of each proxy is constrained by its preservation, post-mortem destruction, and known relationship to sea level.

In tropical coral reef environments, the capacity of coral microatolls to record changes in sea level is well established[19–22]. Microatolls are long-lived coral colonies that develop a discoidal form in intertidal reef settings due to the interplay of the survival constraints of living coral tissue and water level. Corals are limited in their upward growth by exposure during low tide, and consequently, once maximum vertical growth is attained, continued growth is constrained to the outer sides of a colony and lateral growth dominates[23,24]. Based on the close association between coral growth and limiting water level, microatolls have been used as proxy sea level indicators in two primary ways. First, the presence of flat discoidal microatolls have been used to signify past sea level positions. In such studies the precise elevation of microatolls and radiometric dating are used to constrain patterns of sea-level behaviour and sea-level highstands during the Holocene[25–30], and detect changes in water level resulting from storm rubble rampart destruction[31], as well as coseismic activity along tectonically active coasts[32–35]. Second, over shorter timescales, microatolls have been used to resolve interannual and longer-term sea-level behaviour[19,21,36] based on the ability to resolve annual growth properties and observations that short-term changes in water level can be reflected in the surface and skeletal growth response of corals[19]. Indeed, growth patterns have been associated with rising, stable and falling sea levels over decadal to centennial timescales[37]. However, few studies have attempted to extend sea level records using the continuous growth chronology of corals[21]. This in part is attributed to the focus on microatoll specimens from intertidal and emergent reef flats where the vertical growth trajectory is compressed, and samples are diagenetically altered or heavily bioeroded, which can obfuscate the continuous growth signature of corals apart from identification of notable die-down events[28,36].

Here, we present an extended and near-continuous 90-year record (1930–2019) of sea-level behaviour for the central Indian Ocean, that spans the early to late 20th century, from the growth records of a pristine fossil coral microatoll in pedestal growth form, and recent living microatoll that colonised the outer edge of the fossil microatoll (Fig. 1, "Methods"). The height of living coral (HLC) at the study site has a close approximation to mean lowest low water (MLLW, −0.41 m below msl) and this close association to known sea level is examined to reconstruct the change in relative sea level. Our record is based on a methodological development where due to the unique sample quality and preservation of the microatoll, we construct a near-continuous number of sea level minima points (47) and sea level index points (SLIPS, 21) along the growth axis of the coral, which tracks surface morphology and produces highly-resolved sea level data at annual scales. Notably, our sea level reconstruction spans the early 20th to 21st centuries and overlaps the installation of tide gauges in the Maldives archipelago, and extends the observational record by a further six decades. The sea level reconstruction is examined to resolve changes in sea-level behaviour and the onset of the acceleration in sea-level rise in the Indian Ocean.

Results

Growth history of fossil and living coral microatolls

Uranium-Thorium ages indicate the slabbed fossil coral colony captures at least 106 years of growth (1888–1995; Fig. 2b and Supplementary Table 2). Skeletal banding signatures suggest the centre of the slab records the initial stages of vertical growth and transitions to lateral growth around 1900 (Fig. 2b). We reconstruct sea level beginning in 1930 when consistent annual skeletal bands are visible. The surface of the microatoll has minimal bioerosion ("Methods"), an undulating surface, and multiple diedown or negative growth trends (Fig. 2b). Coral growth rate varied along the coral slab with constrained skeletal extension evident during diedown events (mean 1.02 cm.yr^{-1}, range 0.5–1.34 cm.yr^{-1}), and wider growth bands (mean 1.34 cm.yr^{-1}, range 0.78–2.1 cm.yr^{-1}) during periods when the microatoll surface increases in elevation (Supplementary Fig. 5). Lateral growth exceeded or equalled vertical growth in all instances indicating a close coupling of water level to the coral growth surface.

The growth record of this long-lived colony has preserved the impact of a number of climate anomalies during the twentieth century, as recorded in stress signatures that alter coral growth, and reduction in elevation of the height of living coral (Fig. 2). Several climate modes are known to modulate both sea surface temperature and sea level in the Indian Ocean that impact coral growth responses, though the climate processes exhibit significant spatial and temporal variability in the Indian Ocean[10,38–41], and the precise impact on coral growth also varies between events. At the Maldives study location strong El Niño events combined with positive phases of the Indian Ocean Dipole (IOD) can elevate the seasonal peaks in sea surface temperatures (SSTs, Supplementary Fig. 7a), causing widespread coral bleaching, that may result in marked reduction in coral growth, temporary cessation of growth, or coral death (Fig. 2)[42,43]. On the other hand, lower sea level anomalies may occur after negative IOD events[38–41] (Supplementary Fig. 7b) which can promote reduction in the height of living coral tissue and reduction in elevation of the surface of the coral skeleton. Indeed, our coral record also shows multiple die-down episodes that are

https://doi.org/10.1038/s41467-025-60972-2

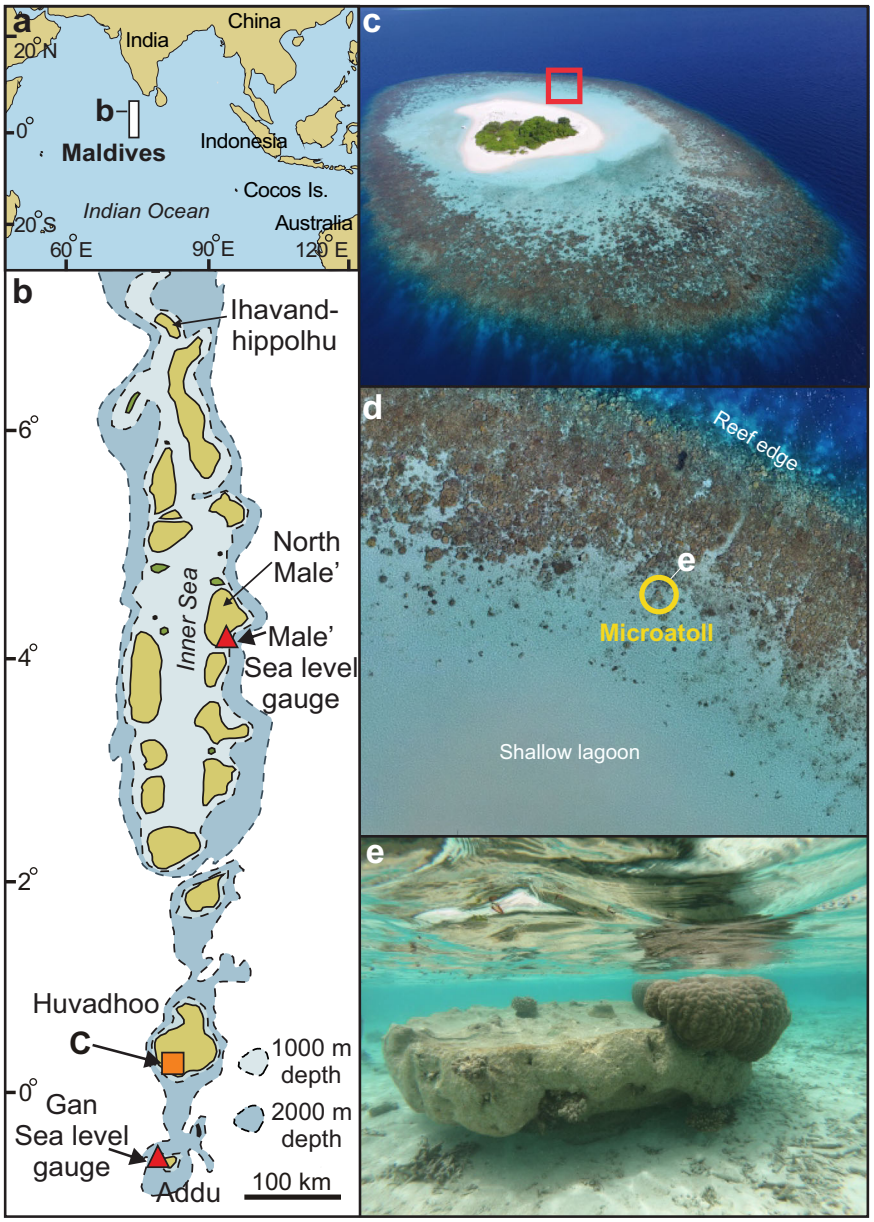

Fig. 1 | Field location of coral microatoll sample site. a Maldives archipelago, central Indian Ocean, source[26]. **b** The Maldives archipelago showing the location of Huvadhoo atoll and position of the Mahutigalaa reef platform, source[26]. **c** Oblique aerial photograph of the Mahutigalaa reef platform. **d** Aerial photograph of the northeastern outer reef showing the position of the sampled microatoll. **e** Image of microatoll at the field site. Note pedestal growth form with base of colony above the current reef surface and recent live coral growth on the outer rim of the colony, highlighting marked increase in sea level from the fossil microatoll edge. See Supplementary Fig. 2 for further details of site characteristics. Source of images (**c**–**e**), lead author.

associated with negative sea level anomalies (Fig. 2, Supplementary Fig. 7b).

Three notable stress events are apparent in the skeletal growth history depicted by the truncation of annual growth bands, followed by regrowth of the colony downwards toward the reef surface. The first two events occurred in 1967–1968 and 1980–1982, respectively, and are temporally proximate with combined El Niño and IOD events. Of note, the 1982 event was closely followed by a negative IOD event, likely inducing a negative sea level anomaly. The third marked stress event, which forced a marked diedown in the height of living tissue between 1992 and 1993, is coincident with an El Niño episode that elevated sea surface temperature in the Maldives 1991/1992[42] followed immediately by a negative phase of the IOD that temporarily lowered sea level (Supplementary Fig. 7b). There is a subsequent further marked reduction in height of living tissue between 1993 and 1995 following the negative IOD event. The colony appears to have died in 1995, as there are no further growth bands present (Fig. 2a, c). Notably, the period in which the coral experienced successive die-downs leading to mortality was coincident with three successive years where maximum low water levels were the lowest on record (Fig. 3b). In total, there are 21 downward growth bands in the coral record.

Following a 12-year hiatus, growth of a new *Porites lutea* colony began on the outer edge and surface of the dead pedestal microatoll (Figs. 1e, 2c). This colony grew vertically between 2006 and 2015 as sea-level rise had opened a depth window across the pedestal surface. In 2015, the new coral colony reached its vertical growth limit and began lateral growth. A significant die-down occurred in 2016, which aligns with the very strong El Niño and global mass coral bleaching event that impacted the Maldives archipelago[43]. This event was associated with a lower sea level as a consequence of the following negative IOD

https://doi.org/10.1038/s41467-025-60972-2

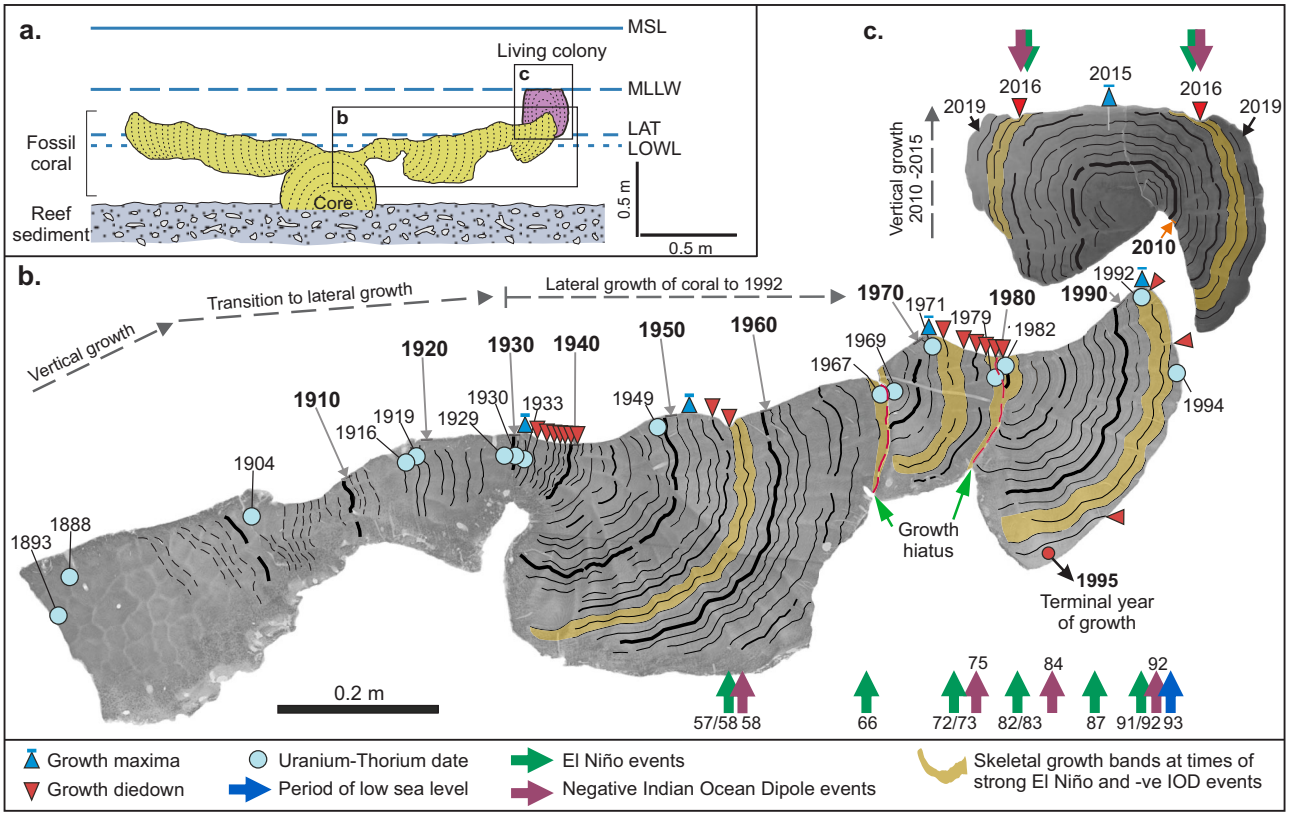

Fig. 2 | Cross-section X-Ray image of pedestal coral, Mahutigalaa reef platform, Huvadhoo atoll. a Schematic cross-section of sampled microatoll showing elevation with respect to known water levels, MSL = mean sea level, MLLW = mean lowest low water, LAT = lowest astronomical tide, LOWL = lowest observed water level. Note the pedestal growth form and colonisation by a living colony on the outer rim. **b** Fossil microatoll slab that lived between 1888 and 1995. Note, annual chronology showing the onset of colony growth pre 1900, transition to lateral growth post 1910 and termination of growth in 1995. **c** Living *Porites lutea* slab on outer edge of pedestal microatoll (See Fig. 1e for growth position). Coral started growth in 2006 and was sampled in February 2020. Note, annual chronology showing the onset of colony growth and vertical growth to reach the limiting water level in 2015, and transition to lateral growth thereafter. Note the die-down associated with the strong negative Indian Ocean Dipole (IOD) event in 2016. Note: die-downs correlate with known strong and very strong El Niño events and strong negative IOD events.

(Figs. 2c, 3a, b and Supplementary Fig. 7b), and confirms the skeletal growth record is responsive to the sea level signal.

90-year sea level reconstruction

The pristine preservation of the coral, lack of bioerosion, comparison of surface topography with growth capacity, and skeletal growth signature that is restrained within its vertical growth capacity by sea level ("Methods") are used to reconstruct a high-fidelity relative sea level record at this tectonically stable location ("Methods", Fig. 3).

Our sea level reconstruction identifies several significant features of sea level behaviour at this locality in the central equatorial Indian Ocean (Fig. 3). First, there is a clear cyclic pattern which has an ~18.6 year frequency, likely driven by the lunar nodal cycle[44] with the maximum amplitude of the lunar diurnal K_1 and O_1 constituents corresponding with higher sea level periods aligned around 1932, 1950/51, 1969, and 1988 (Figs. 2, 3). The coral record also shows sequential years of downward growth in the years preceding the minimum amplitude of the lunar constituents at ~1942, 1960, 1978/79. In particular, the growth record shows eight years of successive downward growth before the 1978/79 minima, and our growth record was truncated by marked die-down (followed by mortality in 1995) three years prior to the 1997 minima.

Due to the equatorial location of our study site in the central Indian Ocean, the amplitude of the nodal tide is expected to be low[45–49], confirmed through analysis of the nodal cycle in our dataset (Methods) indicating an amplitude of ~15 mm. Where we have continuous sea level data (1930–1992), we recalculated rates of sea-level change with the nodal lunar tide removed (NLTR), and we report it alongside estimates based on the raw micro-atoll sea level reconstruction. These results show the nodal cycle has only a small impact on calculations of rates of sea level change.

Second, superimposed on this cyclic pattern, sea level has risen by ~0.174 m between 1930 and 1992, and a further 0.127 m between 1992 and 2019 (total of 0.33 m across the entire record) at rates of 3.06 ± 0.26 mm.y^{-1} (NLTR rate 3.04 ± 0.14 mm.y^{-1}) between 1930 and 1992 (length of primary coral record) and 3.52 ± 0.19 mm.y^{-1} (NLTR rate 3.62 ± 0.17 mm.y^{-1}) across the entire synthesised record (1930–2019). Third, it is apparent that the increase in sea level has not been uniform. The first 30 years of the record (1930–1959) in the early to mid 20th century show a lower rate of sea-level change at ~1.42 ± 0.42 mm.y^{-1} (NLTR rate 1.51 ± 0.33 mm.y^{-1}). From around 1959, the rate of sea-level rise increased to ~3.44 ± 0.68 mm.y^{-1} (NLTR rate 3.07 ± 0.37 mm.y^{-1}, 1960–1992). Between 1990 and 2019 the rate of sea-level rise is ~4.39 ± 0.48 mm.y^{-1}.

Discussion

Our 90-year sea level reconstruction extends the instrumental record by six decades and refines understanding of twentieth-century sea level behaviour in the tropical Indian Ocean. This highly resolved sea level record is based on a methodological refinement that utilises the incremental growth of a coral microatoll. Microatolls have been typically used as markers of sea level position at the colony scale[26], to identify a small number of individual die-down events from a much longer growth record[28,36], or isolate discrete periods of sea level

https://doi.org/10.1038/s41467-025-60972-2

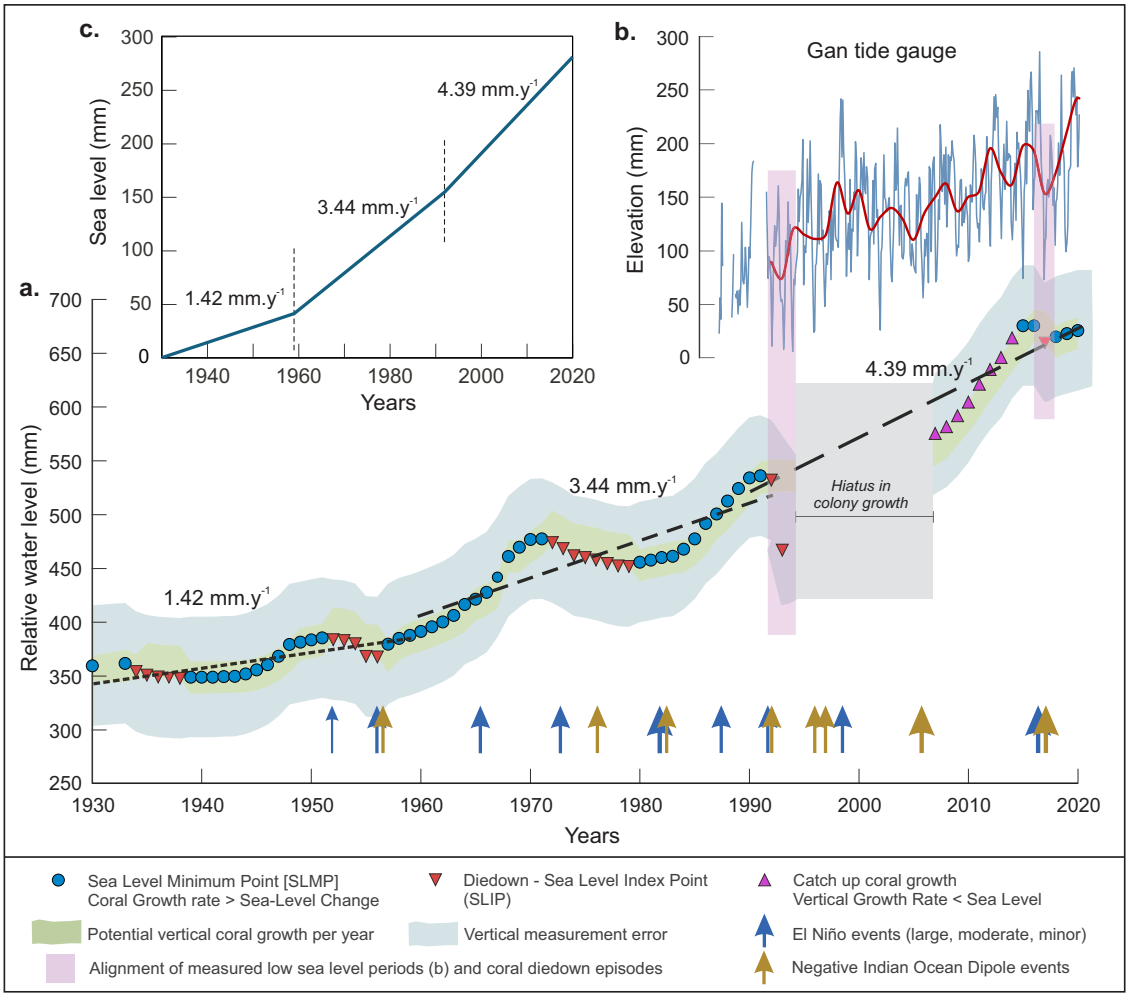

Fig. 3 | 90-year sea level reconstruction for the central Indian Ocean. a Sea level reconstruction from the pedestal microatoll 1930-1992 and modern coral/microatoll growth 2006–2019 (Fig. 2). Dashed lines represented lines of best fit for the periods 1930–1959, 1960–1992, 1990–2019. The source data of annual coral surface elevations are provided in a Source Data file. Source of El Niño data from NOAA (at Climate Prediction Center - ONI (Oceanic Niño Index)) and Indian Ocean Dipole (IOD) data from the Japan Meteorological Agency (at historical IOD events). Note: purple triangles represent the elevation of annual growth bands during catch-up vertical growth of the coral due to relative submergence, as depicted in Supplementary Fig. 6. These points are not an accurate reflection of sea level and were excluded from further analysis of rates of sea-level change. **b** Monthly mean sea level record (1987–2020) from the Gan tide gauge, Addu atoll, 108.45 km south of the field location. PSMSL Station ID 1707, Lat 0.683333° S, Long 73.15°E. The red line is the annual mean sea level. Source: Data and Station Information for GAN II (psmsl.org). **c** Modelled changes in sea level based on trends presented in (a).

variability[19]. We show that where records are largely free of surface and internal bioerosion, it is possible to use coral microatolls as natural archives for near-continuous and fine-scale sea level reconstructions. Such records can be compiled by resolving the precise elevation change of the coral surface between annual growth increments, which capture successive lateral downward and upward growth phases, and that are constrained within the vertical growth potential of the coral[20,35]. Such reconstructions have rarely been attempted due to the relative paucity of extracted long-lived microatolls that span the twentieth century, and the geographic setting and environmental constraints of many sites that impact the preservation of microatoll specimens. For example, many microatolls that grow adjacent to continental landmasses in the tropics (e.g., SE Asia) are located on emergent platforms, and commonly have high rates of internal bioerosion, due to nutrient rich coastal waters, which degrades the skeletal and surface growth signatures, thus limiting their utility for fine-scale sea level reconstructions that span societally relevant timescales. However, at oligotrophic far-field locations, microatolls can remain well-preserved[21], such as the specimen analysed in this study ("Methods", Supplementary Fig. 4).

Our Mahutigalaa coral archive contains a record of sea-level change and climatic variability since the early-mid twentieth century, a critical period of anthropogenically forced global change. The skeletal record contains evidence of multiple separate stress events, recorded as constrained growth bands or die-down episodes, that are temporally coincident with strong El Niño and negative Indian Ocean Diploe (IOD) events since the mid 1950's (Figs. 2 and 3). Marked stress events (three in our record) are likely to reflect short-lived, but distinct, increases in SST associated with El Niño or combined El Niño and IOD events that are responsible for bleaching episodes documented at this location[43]. In addition, temporary lowering of sea level is recorded in the die-down levels of the coral skeletons, where changes in SST may have been below the critical threshold of bleaching. Our record demonstrates that such decadal-scale climate variability, as recorded in the skeletal growth signature of the coral, has had a detectable impact on coral reef ecosystems of the central Indian Ocean since the mid-twentieth century, potentially causing bleaching events prior to more recent observational records over the past four decades, and that widespread bleaching events may possibly have occurred much earlier than commonly assumed[50].

Notably, the fidelity of the coral growth record to sea level variability is validated through overlap of the coral and instrumental records (Fig. 3b). Alignment of diedown episodes associated with elevated SSTs and temporary low sea level positions, as confirmed during the impact of the 2015/2016 El Niño and subsequent negative IOD event (recorded in the Gan water level record, Fig. 3b) on the modern living coral, and close association of other major El Niño and negative IOD events with significant diedown (e.g., 1982, 1992, 1994) demonstrate the temporal connectivity and responsiveness of our coral record to sea level (Supplementary Fig. 7).

Comparison of our 90-year reconstruction from the central Indian Ocean with the longer tide gauge records from coastal sites at Mumbai (India) and Freemantle (Australia) highlights considerable regional variability in sea level behaviour (Fig. 4). First, our reconstruction is broadly consistent with both longer tide gauge records in the early to mid-twentieth century (1930-1950's) that show rates of relative sea-level rise of 2.04 ± 1.9 mm.yr^{-1} and 2.41 ± 1.46 mm.yr^{-1} for Mumbai and Freemantle respectively, though the rate of rise in the Maldives was lower at 1.42 ± 0.42 mm.yr^{-1}. Second, between 1960 and 1992, there is a notable difference in the rate of relative sea-level rise between the central Indian Ocean and sites on continental margins. The Maldives reconstruction indicates a marked increase in the rate of relative sea-level rise across this period to 3.44 ± 0.68 mm.yr^{-1}, compared with the very low rate at Mumbai (0.14 ± 1.08 mm.yr^{-1}) and negative rate at Freemantle (−0.4 ± 1.27 mm.yr^{-1}). Of note, our results differ to previous estimates, based on hybrid reconstruction approaches, that indicated no significant sea level acceleration in the region during this period[4,13,40].

Third, all tide gauge datasets and the coral reconstruction record show the highest rates of sea-level rise post-1990, with the highest rates occurring at the continental margin locations (5.05 ± 1.78 mm.yr^{-1} at Mumbai and 4.66 ± 1.39 mm.yr^{-1} at Freemantle). Based on the elevation difference of the microatoll surface, which terminated growth in 1992, and the elevation of the modern microatoll surface in 2020, sea level has risen ~0.13 m at our location at a rate of 4.39 ± 0.48 mm.yr^{-1} since 1990, though recognising there is a gap in our coral record across that period (Fig. 3). This rate of SLR sits between the two instrumental records in the Maldives, which are 3.37 ± 0.58 mm.yr^{-1} at Gan (south of the field site) and 4.53 ± 0.74 mm.yr^{-1} at Hulhule (north of the field location, Fig. 1) the satellite altimetry record at the study location (Fig. 4). We note that the tide gauge records bounding our site in the Maldives show good consistency with the satellite AVISO record from the area (Fig. 4) and the coral reconstruction represents similar rates of sea level change at this location.

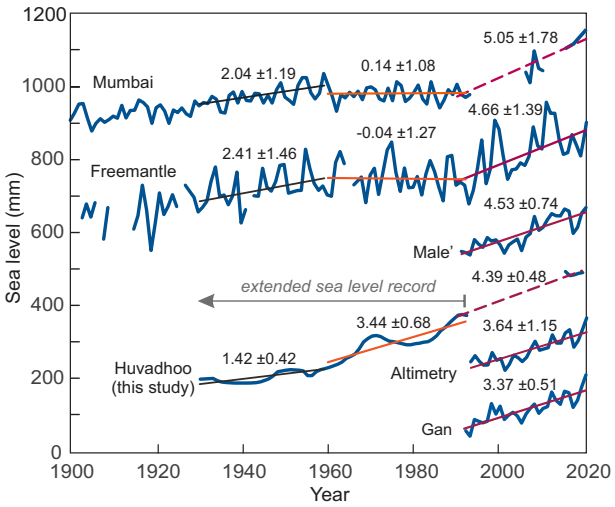

Fig. 4 | Comparison of the longest tide gauge records from the Indian Ocean (Mumbai and Freemantle), with the instrumental tide gauge records from Male' and Gan atolls Maldives and the coral-based sea level reconstruction at Huvadhoo atoll. Data sourced from PSMSL for Mumbai (India Data for MUMBAI / BOMBAY (APOLLO BANDAR)); Freemantle, Australia (Data for FREMANTLE); Male' atoll (Data for MALE-B, HULULE); and Gan (Data for GAN II (psmsl.org)). AVISO Satellite derived sea surface height above geoid for the co-ordinates at the field location. Data source http://ddo-aviso.vlandata.cls.fr:41080/thredds/dodsC/dataset-duacs-rep-global-merged-allsat-phy-l4.

Regional differences in sea level behaviour at decadal timescales, such as those identified in our comparison from the Indian Ocean, have been identified in a number of studies with causes attributed to a range of factors including ice sheet and glacier dynamics, steric and dynamic sea level changes due to climatic variability, earth deformation and vertical land movement[13,39,51–53]. We note that our empirically-based sea level reconstruction from the central Indian Ocean is broadly consistent with recent ensemble reconstructions of GMSL and regional change across the twentieth century[1,4,10,54] though the timing and magnitude of change differ. First, our sea level record shows a lower rate of sea-level rise characterised the early part of the twentieth century (1.42 ± 0.42 mm.y^{-1}). Second, we present observational records for the marked acceleration in the rate of sea-level rise starting in the late 1950's in the central Indian Ocean, slightly before previous estimates[4,40]. We identify an increase in rate of sea-level change (more than doubling to 3.44 ± 0.68 mm.y^{-1}) across the period 1959–1992. Furthermore, our data also show the persistence of this acceleration since the 1960's[4,55]. Third, the rate of sea-level rise has further increased since 1992 (Fig. 4), the period overlapping the instrumental and satellite altimetry period. Our record presents empirical evidence of the previously identified acceleration in SLR in the 1960's.

There are two possible mechanisms that account for the observed earlier onset of accelerated SLR in the Maldives archipelago, and prior to the acceleration as recorded in records from the continental margins (Fig. 4). First, it has been suggested that this acceleration in the Indo-Pacific was primarily due to thermosteric initiation resulting from intensification and basin-scale equatorial shifts in the Southern Hemispheric westerlies. Both reanalyses and climate models show robust intensification of Southern Hemispheric westerlies since the 1950s, responding to anthropogenic forcing such as increasing atmospheric concentrations in greenhouse gases[56,57]. Furthermore, historical data also suggest an equatorward shift in the westerly position, particularly in the southern Indian and Pacific Oceans[4,58]. The intensification of the westerlies enhances the upwelling of cold deep water and thus increases ocean heat uptake, thus contributing to thermosteric sea-level rise[4]. In addition, the strengthening and equatorward shift of the westerly wind stress can increase sea surface slope across the Antarctic circumpolar current, which results in more warm water in the upper oceans pushed northwards and hence a higher rate of sea-level rise in the north[4]. Second, to account for observed spatial differences in the rate of SLR since the 1960's in the Indian Ocean, it has been proposed that the relatively high rate of SLR near the equator could result from surface Ekman mass convergence, caused by an enhanced intertropical convergence zone and a strengthened Indian Ocean Walker cell[13].

Our results and the sea level record produced are unique and further highlight the value of coral archives as recorders of both sea level and climatic variability, which are invaluable in tropical mid-ocean settings to extend spatio-temporally limited instrumental records[19]. The sea level record makes an important contribution in providing empirical data that refines the pattern of sea level behaviour in the central Indian Ocean, and can support refinements and verification of sea-level reconstructions using statistical and reanalysis techniques[7].

Methods

Field setting

A sea-level record was constructed from the skeletal growth patterns archived within a coral microatoll from a reef platform in Huvadhoo atoll, southern Maldives archipelago (Fig. 1a, b). Huvadhoo is the largest and deepest atoll in the Maldives with a perimeter of 261.4 km and an area of 3279 km^2[2,59]. The lagoon is well flushed via numerous deep and wide passages that breach the atoll rim[60]. The sampled microatoll is from the Mahutigalaa lagoonal reef platform located in the southwest sector of the atoll (0°17'22.77"N, 73°12'1.88"E, Fig. 1b, c). Elliptical in shape, the platform is approximately 0.13 km^2 in area, and supports a 0.004 km^2 vegetated island (Supplementary Fig. 2). The topography of the reef platform surface is broadly basin-shaped with a higher elevation outer rim (~0.4 m below mean sea level (MSL)) and shallow inner platform (0.4–1.5 m below MSL). The reef surface can be divided into four major eco-geomorphological zones, which vary in width around the platform[61] (Supplementary Fig. 2b). (1) The outer reef edge (20–80 in width) incorporates the transition to the forereef slope and comprises a dense and complex in situ reef framework of live coral (~10–30% cover and predominantly of massive morphology) and dead coral (~30–50% cover). (2) The outer reef margin transitions to a narrow inner reef (10–30 m wide) comprising an open framework of living coral (10–30% cover, predominantly of massive morphology) and dead coral (20–40%) that ranges in elevation from −0.5 to −0.8 m MSL. This zone has dense microatoll growth forms (*Porites* spp. and *Heliopora coerulea*) and is the location of the sample cut and analysed in this study. Of note, in this zone, there are multiple specimens similar to that analysed in this study. (3) The reef flat surface grades into a patch reef zone (−0.8 m to −1.2 m MSL) that ranges in width from 20 to 90 m around the platform and is characterised by a mixed rubble and sand substrate (60–80%) with isolated coral patches, including microatolls. (4) The inner reef platform is a shallow trough, 20 to 100 m wide, that encircles the vegetated sand cay and is composed of medium-fine sized sand.

Fields of fossil *Porites* spp. microatolls have previously been described on the central reef platform, occupying the sandy trough and coral patch zones[26] (Supplementary Fig. 2a). This study examines the growth record preserved in a modern microatoll (~100 years in age) from the inner reef zone (Supplementary Fig. 2b). The microatoll is 2.7 m diameter and has a characteristic discoidal shape, and near planar surface, consistent with lateral growth morphology under constrained sea-level conditions (Fig. 1e).

The southern Maldives provides a suitable environment that maximises the potential use of microatolls to detect sea level changes[37]. First, the 850 km long archipelago is located in a tectonically stable setting midway along the Laccadive-Chagos aseismic submarine ridge[62,63]. Second, the atoll experiences a microtidal regime (mean neap and spring tide range of ~0.4 m and 1.1 m, respectively), with low amplitude annual variations in sea level, which enhances the sensitivity of microatolls to sea level change[19,21]. Third, as Mahutigalaa is located 11 km inside the atoll periphery, it is protected from direct oceanic swell impact. Consequently, incident wave energy is low to moderate as it can only be impacted by residual ocean swell that propagates through passages in the reef rim, and internal lagoon-generated waves. Due to the low energy character of the wave regime impacting the platform, significant wave-driven differences in water level that can influence variations in microatoll growth in larger and higher energy reef systems are considered negligible at the study site. Fourth, the equatorial setting implies that high-energy storm events, that can physically impact and mobilise coral colonies or induce moating through deposition of rubble tracts, are rare[23,26]. Fifth, the Mahutigalaa platform is free draining at the current sea level and ponding is not apparent as demonstrated through surveys of the height of living microatolls.

Instrumental sea level records

Sea-level records are available from satellite data, and two tide gauges located 432 km north (Hulhule, Male' atoll) and 108 km south (Gan, Addu atoll) of the Mahutigalaa reef platform (Supplementary Fig. 3). Consistent data from these sources begins around 1990 and reveal an increase in sea-level over the past 3 decades, with rates of 3.37 ± 0.58 mm.y^{-1} at Gan to 4.53 ± 0.74 mm.y^{-1} at Male'. The satellite altimeter record for the field location (Supplementary Fig. 3a) also shows an increase in sea level of 3.71 mm.y^{-1}.

Microatoll sampling

We sampled a dead *Porites lutea* microatoll on the freely draining northeastern side of the Mahutigalaa reef platform at the transition of the outer reef flat to inner reef zone (0°17'22.77"N, 73°12'1.88"E, Fig. 1 and Supplementary Fig. 2). The microatoll was 2.7 m in diameter and assumed a pedestal growth form in which the colony grew from its core and subsequently transitioned to lateral growth over the reef and sediment surface (Fig. 2). The outer margin of the colony was 0.632 m above the bed with a 0.2 m gap between the sediment surface and underside of the colony (Fig. 2a). A living *Porites lutea* coral colony was growing on the outer edge and surface of the larger dead microatoll (Figs. 1e, 2a, c). A 10 cm-wide slab was cut using handsaws along the radius of the microatoll beginning at the island-facing outer edge (Fig. 2). A 10 cm wide slab was also cut from the living colony growing on the outer margin of the microatoll.

Prior to slabbing, laser level surveys (error of ± 2 cm) were undertaken to determine the elevation of the outer and inner margins of the slab relative to sea level. Surveys of the height of 30 living microatolls were also undertaken to determine the variability in height of living coral (range 9.5 cm ± 2.3 cm SD). All survey data was reduced to sea level based on the known elevation of benchmarks in the island surface using the tidal datums calculated from the Gan sea level records (UHSLC Stations (hawaii.edu)). Analysis of this data indicates the height of living coral is −0.42 m ± 0.03 m below MSL, which is a close approximation to MLLW (−0.41 m msl).

Slab processing and establishment of the growth chronology

The slab was recut into a 0.7 cm slice, using a 0.45 mm diamond wire saw. An X-ray image was captured at 50 kV, 10 mAs with a source-to-object distance of 1 m and an exposure time of 20 msec at the Diagnostic Imaging Laboratory at National University Hospital, Singapore. An annual growth chronology for the slab was constructed based on the converted annual skeletal density growth bands from the X-ray images[64] using ImageJ, and temporally constrained by disequilibrium Uranium-Thorium ages (^{230}Th ages).

Nineteen Uranium-Thorium dates (including two replicates) were obtained along the slab in order to determine the time window of coral growth, refine ages of highest and lowest levels of colony growth, and resolve age disparities either side of apparent stress events in the skeletal growth record (Supplementary Table 2). Samples were gently crushed into 1 to 3 mm^3 segments. Clean and pristine pieces were selected under a microscope, and subsequently ultrasonically cleaned (three times) in superclean water. For each sample, 30 to 60 mg was used for U-Th chemistry[65]. All samples were dissolved in ultrapure nitric acids, and a ^{229}Th-^{233}U–^{236}U mixed spike was then added to the solutions. $HClO_4$ was also added to remove organic compounds. Each sample solution was refluxed at 175 °C for 2 h and dried. Samples were re-dissolved by adding 2 N ultrapure HCl solution. Co-precipitation was achieved by adding $FeCl_3$ and concentrated NH_4OH. Co-precipitates were re-dissolved and put through an anion-exchange resin in columns to separate and purify uranium and thorium. U and Th fractions were then dissolved in 1% HNO_3 (+ 0.1% HF) for instrumental analysis. U and Th isotopic compositions were determined on a multi-collector inductively coupled plasma mass spectrometer (MC-ICP-MS, a Neptune Plus from Thermo Fisher Scientific) at the Earth Observatory

of Singapore and Asian School of the Environment (ASE), Nanyang Technological University, Singapore. The measurements were undertaken using a recently improved SEM peak-jumping technique[66,67]. Uncertainties in the U and Th isotopic data and ^{230}Th dates are quoted at the 2σ level in this paper.

Microatoll bioerosion

Bioerosion can have a significant impact on the surface and internal structure of coral microatolls and subsequent reconstructions of sea level. We quantified the degree of bioerosion of the coral slab using digital analysis of the proportion of the slab that had undergone boring (erosion holes, boring tunnels) relative to total slab area. The analysis examined both bioerosion signatures on the surface and underside of the coral. Boring holes and tunnels, and sections of the slabs (e.g., surface and underside) where skeletal banding was visibly speckled, most likely by CCA overgrowth (Supplementary Fig. 4), were segmented using the Magnetic Lasso tool in Adobe Photoshop. Segmented pixels were quantified against the total pixel area of each slab and the total area of the coral sample (Supplementary Table 3). The images were not enhanced prior to analysis.

Overall, 20% of the coral slab had been affected by bioerosion. Bioerosion was most prevalent on the underside of the slab (17.8%) and on older central portions of the coral which was continuously in contact with the sediment surface (Supplementary Fig. 4). Notably, only 2.3% of the upper surface was affected by bioerosion, and excluding the central section (which was not used in this study for sea level reconstruction), the remaining surface of the coral had only 0.91% bioerosion. Notably, this portion of the slab was perched above the sediment surface at the time of slabbing. We conclude the surface of the coral used for sea level reconstruction was remarkably well preserved.

Reconstruction of water level

Reconstruction of water level changes were based on the elevation of the coral growth surface relative to sea level as measured from the continuous growth record of the microatoll surface and observed die-downs in skeletal bands. We note the pristine nature of our sample, with negligible bioerosion of the coral surface that shows a continuous record of coral growth and incremental transitions between upward growth and several die-down periods (Fig. 2). To resolve changes in surface elevation of growth bands, the x-ray image was analysed digitally. Field survey data of slab elevation was used as control points to rectify the image to the correct horizontal and vertical orientation, as the in-situ slab. The rectified image was imported into the Matlab function *grabit.m*[68] and calibrated to the known x- and y-scale. Each annual growth band was digitised based on the highest level of coral growth observed within each band. Digitising precision is estimated at 0.5 mm, and error is estimated at ± 0.3 mm, calculated as the mean absolute error between repeat digitising of an individual line. Digitised points were saved for each annual increment and transformed to the sea level datum.

Inferring water levels from skeletal growth signals. Microatolls preserve a low-frequency record of the water level that constrains upward coral growth (e.g., MLLW), and therefore is not a record of mean sea level[20]. Interpretation of water level responses from the skeletal record must be undertaken with great care (Supplementary Fig. 6). When a microatoll experiences an extreme low water level, the coral tissue can be stressed, and those parts of the coral tissue at highest elevation can die. At these times, lower water level limits the highest level of survival (HLS). Such 'diedown' events are expressed as a reduction in elevation of the coral growth surface (Supplementary Fig. 6). Our complete record contains 21 years when the surface of the coral and skeletal bands signify reduction in elevation from previous years (Fig. 2). These diedown elevations are considered to robustly reflect sea level limiting points and are used to construct sea level index points (SLIPS)[37]. Conversely, when a microatoll experiences higher than normal low water levels, the coral tissue can grow vertically. The height to which the coral can grow is limited by the colony vertical growth capacity (VGC). Analysis of the annual skeletal growth record in the microatoll sample showed the microatoll had a mean growth rate of 14.0 ± 0.39 mm.y^{-1} and ranged from 9.1 to 28.3 mm.y^{-1} (Supplementary Fig. 5). The mean value is similar to that previously identified for *Porites* corals in the Maldives[69]. We adopt this mean value as the VGC for the microatoll. In circumstances where the increase in water level is larger than the VGC the coral surface decouples from the low water level signal and there is a temporal lag before the growth of the coral surface catches up to water level (Supplementary Fig. 6). During this lag period the coral surface is submerged beneath the limiting water level (e.g., by ~0–10 cm, Supplementary Fig. 6) and the surface topography does not provide a precise characterisation of water level (TWL > VGC). At best, the microatoll surface presents a conservative lower estimate of water level position. However, where the VGC ≥ SLR the coral surface can remain coupled to its limiting water level and therefore provides a more continuous record of water level behaviour (Supplementary Fig. 6). Significantly, at no stage in our longer slab record did the vertical growth exceed the lateral growth capacity of the colony suggesting the coral surface is likely to reflect a close association with water level change. We identify 48 years of incremental upward growth that represent the highest level of growth (HLG) of coral tissue and are used to reconstruct sea level minimum points[37,70,71]. We note that the annual incremental growth in our record falls well within the annual growth rate of *Porites lutea* from the field site[69].

The outer living coral slab began growing in submerged conditions and both the skeletal growth signature and growth rates from 2006-2014 indicate upward growth dominated (Fig. 2c). These years of growth are not reliable indicators of water level as the coral was in catch-up growth mode (e.g., Supplementary Fig. 6 and purple triangles in Fig. 3). These datapoints are excluded from analysis of sea level change. However, the period from 2015–2020 is characterised by lateral growth as the colony was coupled to its limiting water level (Figs. 2c, 3a).

Evaluating uncertainties

We reconstruct a relative sea level history from the skeletal signatures of the fossil coral (sea level index points and sea level minima points), which in our record terminate at the height of living coral (HLC) in 2019. Total elevation uncertainty is estimated from the expression $Ei = (e1^2 + e2^2 + en^2)^{1/2}$, where e1…en are individual sources of error for sample *i*. Our sea level reconstruction considers four sources of uncertainty. (1) Variability in the Height of Living Coral (HLC). This biological elevation reference was established based on surveys of the elevation of the living upper surface of 30 live *Porites* spp. located within 50 m of the pedestal coral location. At each coral, a minimum of five elevation points were recorded around each specimen to account for within colony variability. The elevation range of the upper surface of living *Porites* colonies was 9.5 cm ± 2.3 cm, and we adopt the standard deviation of the observations (± 2.3 cm). The low range of growth elevations is consistent with other studies of microatolls in microtidal settings[20,36]. (2) Uncertainty from surveying the elevation of the coral microatolls with a laser level (± 2.0 cm). (3) Uncertainties in digitising to reconstruct the coral surface (±0.05 cm). (4) Uncertainty associated with surface bioerosion. As analysis of the pedestal slab showed minimal surface bioerosion along the sector of the sample used to reconstruct sea level (Supplementary Fig. 4 and Supplementary Table 3) we adopt a conservative value of ±1.0 cm. This value is lower than that used in previous studies, where the coral surfaces are heavily bioeroded. Consequently, we estimate the total elevation uncertainty of our record at ±3.21 cm.

As the study focusses on sea level behaviour over the past 100 years, we present the relative sea level change as recorded within the skeletal record. While we do not attempt to transfer our record to an absolute sea level datum, we compare our HLC measurements to the known tidal datum at Gan based on fixed benchmarks on the island. We estimate our HLC level equates to a tidal value of −0.42 m ± 0.03 m below MSL. This elevation is a close approximation to MLLW (−0.41 m).

Removal of lunar nodal tide cycle

Following the identification of the 18.6-year nodal lunar tide in the coral sea level reconstruction, we explored its influence on estimated rates of sea-level rise. Our study site is located near the equator in the central tropical Indian Ocean. Although it remains debated the extent to which the 18.6-yr nodal cycle follows the equilibrium law, the amplitude of the nodal tide at the Maldives study location is expected to be less than 20 mm[45–48]. We removed the lunar nodal cycle signal from our microatoll-based sea level record. First, we performed polynomial regression on the sea level record to estimate the nodal tide cycle ($R^2 = 0.98$). The obtained cycle peaks at around 1933, 1952, 1970 and 1989, consistent with the relatively high sea level points around 1932, 1950/51, 1969 and 1988 observed in the microatoll (Fig. 2), as well as the calculated timing based on the equilibrium law[72]. The cycle has an amplitude of ~15 mm on yearly averaged sea level variation, which approximates the theoretical value of ~9 mm derived from the equilibrium law[48].

We then removed the nodal tide cycle from the original data and recalculated rates of sea-level rise. Results showed only marginal differences in sea-level rise estimates before and after correcting the nodal cycle. For example, for the period 1930-1992 calculated rates of sea-level rise were 3.06 ± 0.26 mm.y^{-1} from the raw dataset and 3.04 ± 0.18 mm.y^{-1} when the nodal lunar tide cycle was removed (a difference of −0.02 mm.y^{-1}). Between 1930 and 2019, the estimated values were 3.52 ± 0.19 mm.y^{-1} (raw data) and 3.62 ± 0.17 mm.y^{-1} (nodal lunar tide removed) a difference of 0.1 mm.y^{-1}. These results show the nodal cycle has only a small impact on calculations of rates of sea level change. However, we note that our dataset has a significant gap (1995–2015), which increases the uncertainty of corrected sea-level rise estimates in this period. Consequently, where we have continuous sea level data (1930–1992), we recalculated rates of sea-level change with the nodal lunar tide removed (NLTR), and we report it alongside estimates based on the raw micro-atoll sea level reconstruction.

Data availability

Data generated or analysed in this study are included in the published article, its supplementary information file, and a Source Data file. The data in Fig. 3a is available as a Source Data file. Source data are provided in this paper.

References

1. Palmer M.D. et al. ensemble approach to quantify global mean sea-level rise over the 20th century from tide gauge reconstructions. *Env. Res. Lett.* **16**, 044043 (2021).
2. Slangen, A. B. A. et al. Evaluating model simulations of twentieth-century sea level rise. Part I: Global mean Sea Level Change. *J. Clim.* **30**, 8539–8563 (2017).
3. Meyssignac, B. et al. Evaluating model simulations of twentieth-century sea-level rise. Part II: Regional Sea-Level Changes. *J. Clim.* **30**, 8565–8593 (2017).
4. Dangendorf, S. et al. Persistent acceleration in global sea-level rise since the 1960s. *Nat. Clim. Change* **9**, 705–710 (2019).
5. Dieng, H. B., Cazenave, A., Meyssignac, B. & Ablain, M. New estimate of the current rate of sea level rise from a sea level budget approach. *Geophys. Res. Lett.* **44**, 3744–3751 (2017).
6. Nerem, S. et al. Climate change driven accelerated sea level rise detected in the altimeter era. *Proc. Natl. Acad. Sci. USA* **115**, 2022–2025 (2018).
7. Carson, M. et al. Regional sea level variability and trends, 1960–2007: A comparison of sea level reconstructions and ocean syntheses. *J. Geophys. Res. Oceans* **122**, 9068–9091 (2017).
8. Douglas, B. C. Global sea level rise. *J. Geophys. Res.* **96**, 6981–6992 (1991).
9. Ponte, R. M. et al. Towards comprehensive observing and modeling systems for monitoring and predicting regional to coastal sea level. *Front. Mar. Sci.* **6**, 437 (2019).
10. Frederikse, T. et al. The causes of sea-level rise since 1900. *Nature* **584**, 393–397 (2020).
11. Frederikse, T., Jevrejeva, S., Riva, R. E. M. & Dangendorf, S. A. consistent sea-level reconstruction and its budget on basin and global scales over 1958–2014. *J. Clim.* **31**, 1267–1280 (2018).
12. Dangendorf, S. et al. Reassessment of 20th century global mean sea level rise. *Proc. Natl. Acad. Sci. USA* **114**, 5946–5951 (2017).
13. Han, W. et al. Patterns of Indian Ocean sea-level change in a warming climate. *Nat. Geosci.* **3**, 546–550 (2010).
14. Woodworth, P. L. et al. Evidence for the accelerations of sea level on multi-decade and century timescales. *Int. J. Climatol.* **29**, 777–789 (2009).
15. Cazenave, A. & Cozannet, G. L. Sea level rise and its coastal impacts. *Earth's Future* **2**, 15–34 (2014).
16. Perry, C. T. et al. Loss of coral reef growth capacity to track future increases in sea level. *Nature* **558**, 396–400 (2018).
17. Saintilan, N. et al. Widespread retreat of coastal habitat is likely at warming levels above 1.5 °C. *Nature* **621**, 112–119 (2023).
18. Horton, B. P. et al. Mapping sea-level change in time, space, and probability. *Annu. Rev. Environ. Resour.* **43**, 481–521 (2018).
19. Woodroffe, C. D. & McLean, R. F. Microatolls and recent sea level change on coral atolls. *Nature* **344**, 531–534 (1990).
20. Smithers, S. G. & Woodroffe, C. D. Microatolls as sea-level indicators on a mid-ocean atoll. *Mar. Geol.* **168**, 61–78 (2000).
21. Smithers, S. G. & Woodroffe, C. D. Coral microatolls and 20th century sea level in the eastern Indian Ocean. *Earth Planet. Sci. Lett.* **191**, 173–184 (2001).
22. Yu, K.-F., Zhao, J.-X., Done, T. & Chen, T.-G. Microatoll record for large century-scale sea-level fluctuations in the mid-Holocene. *Quat. Res.* **7**, 354–360 (2009).
23. Scoffin, T. P. & Stoddart, D. R. The nature and significance of microatolls. *Philos. Trans. R. Soc. Lond. Ser. B* **284**, 99–122 (1978).
24. Stoddart, D. R. & Scoffin, T. P. Microatolls: Review of form. origin, and terminology. *Atoll Res. Bull.* **228**, 17 (1979).
25. Kench, P. S. et al. Holocene reef growth in the Maldives: evidence of a mid-Holocene sea level highstand in the central Indian Ocean. *Geol* **37**, 455–458 (2009).
26. Kench, P. S. et al. Marked sea level variability in the Indian Ocean over the past two millennia. *Nat. Geo.* **13**, 61–64 (2020).
27. Mann, T. et al. Holocene sea levels in Southeast Asia, Maldives, India and Sri Lanka: the SEAMIS database. *Quat. Sci. Rev.* **219**, 112e125 (2019).
28. Meltzner, A. J. et al. Half-metres sea-level flucturations on centennial timescales from mid-Holocene corals of Southeast Asia. *Nat. Commun.* **8**, 14387 (2017).
29. Mann, T. et al. Fossil Java Sea corals record Laurentide ice sheet disappearance. *Geol* **51**, 631–636 (2023).
30. Yan, T., Yu, K., Jiang, L., Li, Y. & Zhao, N. Significant sea-level fluctuations in the western tropical Pacific during the mid-Holocene. *Paleoceanogr. Paleoclimatol.* **39**, e2023PA004783 (2024).
31. Hopley, D. & Isdale, P. Coral micro-tolls, tropical cyclones and reef flat morphology: a north Queensland example. *Search* **8**, 79–81 (1977).

32. Natawidjaja, D. H. et al. Source parameters of the great Sumatran megathrust earthquakes of 1797 and 1833 inferred from coral microatolls. *J. Geophys. Res.* **111**, B06403 (2006).
33. Natawidjaja, D. H. et al. Interseismic deformation above the Sunda megathrust recorded in coral microatolls of the Mentawai islands, West Sumatra. *J. Geophys. Res.* **112**, B02404 (2007).
34. Meltzner, A. J. et al. Coral evidence for earthquake recurrence and an A.D. 1930-1455 cluster at the south end of the 2004 Aceh-Andaman rupture. *J. Geophys. Res.* **115**, B10402 (2010).
35. Debaecker, S. et al. Recent relative sea-level changes recorded by coral microatolls in Southern Ryukyus islands, Japan: Implication for the seismic cycle of the megathrust. *Geochem. Geophys. Geosyst.* **24**, e2022GC010587 (2023).
36. Majewski, J. M. et al. Extending instrumental sea-level records using coral microatolls, an example from Southeast Asia. *Geophys. Res. Lett.* **49**, e2021GL095710 (2022).
37. Meltzner, A. J., Woodroffe, C. D. *Handbook of Sea-Level Research*. (2015).
38. Aparna, S. G., McCreary, J. P., Shankar, D. & Vinayachandran, P. N. Signatures of Indian Ocean dipole and El Niño–Southern Oscillation events in sea level variations in the Bay of Bengal. *J. Geophys. Res.* **117**, C10012 (2012).
39. Han, W. et al. Spatial patterns of sea level variability associated with natural internal climate modes. *Surv. Geophys.* **38**, 217–250 (2017).
40. Palanisamy, H. et al. Regional sea level variability, total relative sea level rise and its impacts on islands and coastal zones of Indian Ocean over the last sixty years. *Glob. Planet. Change* **116**, 54–67 (2014).
41. Han, W. et al. Impacts of basin-scale climate modes on coastal sea level: A review. *Surv. Geophys.* **40**, 1493–1541 (2019).
42. Edwards, A. J. et al. Coral bleaching and mortality on artificial and natural reefs in Maldives in 1998, sea surface temperature anomalies and initial recovery. *Mar. Poll. Bull.* **42**, 7–15 (2001).
43. Perry, C. T. & Morgan, K. M. Bleaching drives collapse in reef carbonate budgets and reef growth potential on southern Maldives reefs. *Sci. Reps.* **7**, 1–9 (2017).
44. Loder, J. W. & Garrett, C. The 18.6-year cycle of sea surface temperature in shallow seas due to variations in tidal mixing. *J. Geophys. Res.* **83**, 1967–1970 (1978).
45. Osafune, S. & Yasuda, I. Numerical study on the impact of the 18.6-year period nodal tidal cycle on water masses in the subarctic North Pacific. *J. Geophys. Res.* **117**, C05009 (2012).
46. Proudman, J. The condition that a long-period tide shall follow the equilibrium law. *Geophys. J. Roy. Astron. Soc.* **3**, 244–249 (1960).
47. Houston, J. R. & Dean, R. G. Accounting for the Nodal Tide to improve estimates of Sea level acceleration. *J. Coast. Res.* **27**, 801–807 (2011).
48. Woodworth, P. L. A note on the Nodal Tide in Sea level records. *J. Coast. Res.* **28**, 316–323 (2012).
49. Bult, S. V., Le Bars, D., Haigh, I. D. & Gerkema, T. The effect of the 18.6- year lunar nodal cycle on steric sea level changes. *Geophys. Res. Lett.* **51**, e2023GL106563 (2024).
50. Hughes, T. P. et al. Global warming and recurrent mass bleaching of corals. *Nature* **543**, 373–377 (2017).
51. Woodworth, P. L. et al. Forcing factors affecting Sea level changes at the coast. *Surv. Geophys.* **40**, 1351–1397 (2019).
52. Zanna, L. et al. Global reconstruction of historical ocean heat storage and transport. *Proc. Natl. Acad. Sci. USA* **116**, 1126–1131 (2019).
53. Hamlington, B. D. et al. Understanding of contemporary regional Sea-level change and the implications for the future. *Rev. Geophys.* **58**, https://doi.org/10.1029/2019rg000672 (2020).
54. Fox-Kemper, B. et al. *Ocean, cryosphere and Sea Level Change* (2021).
55. Church, J. et al. Sea Level Change. in *Climate Change 2013: The Physical Science Basis. Contribution of Working Group I to the Fifth Assessment Report of the Intergovernmental Panel on Climate Change* (eds. Stocker, T. F. et al.) 1137–1216 (Cambridge University Press, 2013).
56. Bouttes, N., Gregory, J. M., Kuhlbrodt, T. & Suzuki, T. The effect of windstress change on future sea level change in the Southern Ocean. *Geophys. Res. Lett.* **39**, L23602 (2012).
57. Frankcombe, L. M., Spence, P., Hogg, A. M. C. O., England, M. H. & Griffies, S. M. Sea level changes forced by Southern Ocean winds. *Geophys. Res. Lett.* **40**, 5710–5715 (2013).
58. Swart, N. C. & Fyfe, J. C. Observed and simulated changes in the Southern Hemisphere surface westerly wind-stress. *Geophys. Res. Lett.* **39**, L16711 (2012).
59. Naseer, A. & Hatcher, B. G. Inventory of the Maldives coral reefs using morphometrics generated from Landsat ETM+ imagery. *Coral Reefs* **23**, 161–168 (2004).
60. Aslam, M. & Kench, P. S. Reef Island dynamics and mechanisms of change: Huvadhoo atoll, Republic of Maldives, Indian Ocean. *Anthropocene* **18**, 57–88 (2017).
61. Ryan, E. J., Hanmer, K. & Kench, P. S. Massive corals maintain a positive carbonate budget of a Maldivian upper reef platform despite major bleaching event. *Sci. Rep.* **9**, 6515 (2019).
62. Rovere, A., Khanna, P., Bianchi, C. N., Droxler, A. W., Morri, C. & Naar, D. F. Submerged reef terraces in the Maldivian Archipelago (Indian Ocean). *Geomorph* **317**, 218–232 (2018).
63. Ling, A. et al. Middle Miocene platform drowning in the Maldives associated with monsoon-related intensification of currents. *Palaeogeogr. Palaeoclimatol Palaeoecol.* **567**, 110275 (2021).
64. Carricart-Ganivet, J. P. & Barnes, D. J. Densitometry from digitized images of X-radiographs: methodology for measurement of coral skeletal density. *J. Ex. Mar. Biol. Ecol.* **344**, 67–72 (2007).
65. Shen, C. C. et al. High-precision and high-resolution carbonate 230 Th dating by MC-ICP-MS with SEM protocols. *Geochim. Cosmochim. Ac.* **99**, 71–86 (2012).
66. Cheng, H. et al. Improvements in 230Th dating, 230Th and 234U half-life values, and U–Th isotopic measurements by multi-collector inductively coupled plasma mass spectrometry. *Earth Planet. Sci. Lett.* **371**, 82–91 (2013).
67. Chiang, H. W., Lu, Y., Wang, X., Lin, K. & Liu, X. Optimizing MC-ICP-MS with SEM protocols for determination of U and Th isotope ratios and 230Th ages in carbonates. *Quat. Geochronol.* **50**, 75–90 (2019).
68. Jiro, GRABIT, MATLAB Central File Exchange. Retrieved February **12**, (2018).
69. Morgan, K. M. & Kench, P. S. Skeletal extension and calcification of reef-building corals in the central Indian Ocean. *Mar. Env. Res.* **81**, 78–82 (2012).
70. Van de Plassche O. (Ed.) *Sea-Level Research: A Manual for the Collection and Evaluation of Data*. (1986).
71. Taylor, F. W., Frohlich, C., Lecolle, J. & Strecker, M. Analysis of partially emerged corals and reef terraces in the central Vanuatu arc: comparison of contemporary coseismic and conseismic with Quaternary vertical movements. *J. Geophys. Res.* **92**, 4905–1933 (1987).
72. Pugh, D. T. *Tides, Surges and Mean Sea-Level: A Handbook for Engineers and Scientists*. (1987).

Acknowledgements

We acknowledge LaMer Group and the Small Island Research Centre, Fares-Maathodaa, Huvadhoo atoll for logistical support, Government of the Maldives for research permission under the Ministry of Fisheries and Agriculture permit numbers 30-D/INDIV/2018/28, and 30-D/INDIV/2020/7. We thank Eddie Beetham, Tracey Turner, Briar, Jacob and Joshua Kench for field assistance. X.W. acknowledges the financial support from the Singapore Ministry of Education under grant numbers MOR-T2EP10122 and MOE-MOET32022-0006.

Author contributions

P.K. conceived the project. P.K. and S.O. undertook fieldwork. X.W. and L.K. performed U-Th dating; K.M., K.L. and R.R. undertook x-ray and bioerosion analysis of the coral sample. P.K., K.M. and S.O. led manuscript development and interpretation. P.K., X.W., K.M. and S.O. contributed to manuscript revision.

Competing interests

Authors declare no competing interests.

Additional information

Supplementary information The online version contains supplementary material available at https://doi.org/10.1038/s41467-025-60972-2.

Correspondence and requests for materials should be addressed to Paul S. Kench.

Peer review information *Nature Communications* thanks Hajime Kayanne and the other anonymous reviewer(s) for their contribution to the peer review of this work. A peer review file is available.